ICAS 2021 SHANGHAI
32nd Congress of the International Council of the Aeronautical Sciences
September 6-10, 2021 Pudong Shangri-La, Shanghai, China

Sparse Polynomial Chaos Expansion based on Fully Adaptive Forward-Backward Selection Method

Huan Zhao[1], Zheng-hong Gao[2], Lu Xia[2]

[1]School of Aeronautics and Astronautics, Sun Yat-sen University, Guangzhou, 510275, P. R. China
[2]School of Aeronautics, Northwestern Polytechnical University, Xi'an Shaanxi, 710072, P. R. China

Abstract

Uncertainties consequentially exist in almost all of engineering and physical problems. These uncertainties may cause the system performance to change or fluctuate, or even cause severe deviation and result in unanticipated or even unprecedented function fault and mission failure. As an efficient uncertainty quantification (UQ) methodology for moment propagation and probability analysis of quantities of interest (QoI's), polynomial chaos (PC) expansions have received broad and sustained attentions. However, the exponentially increasing cost of building PC representations with increasing dimension of uncertainty, i.e., the curse of dimensionality, seriously restricts the practical application of PC at the industrial level. Some efficient strategies applying adaptive basis selection algorithm for sparse optimization (or l_1-minimization) of PC show great potential compared to the classical full PC. However, these strategies mainly focus on forward selection algorithms, which are incapable of correcting any error made by these algorithms. Hence, a novel adaptive forward-backward selection (AFBS) algorithm has been developed for reconstructing sparse PC. The proposed algorithm by a reasonable combination of forward selection and adaptively backward elimination technique can efficiently correct mistakes made by earlier forward selection steps, which retains the most significant PC terms and discards redundant or insignificant ones. The proposed algorithm was first proposed in reference (Zhao, H., Gao, Z., et al. "An efficient adaptive forward–backward selection method for sparse polynomial chaos expansion," Computer Methods in Applied Mechanics and Engineering Vol. 355, 2019, pp. 456-491.). In this paper a fully adaptive forward-backward selection (FAFBS) algorithm is proposed by involving an efficient optimization search algorithm for adaptively selecting the optimal sparse PC. The developed FAFBS method is investigated by several analytical functions and a challenging aerodynamic analysis application. The results demonstrate that the proposed FAFBS method can efficiently identify the significant PC contributions describing the problems, and reproduce sparser PC metamodel and more accurate UQ results than classical orthogonal matching pursuit (OMP) and full PC methods.

Keywords: uncertainty quantification; sparse polynomial chaos; adaptive forward-backward selection; fully adaptive forward-backward selection; aerodynamic analysis

1. Introduction

Uncertainties consequentially exist in almost all of engineering and physical problems. These uncertainties may lead to the system performance to change or fluctuate, or even cause severe deviation. Deterministic approaches may not always converge to the desired optima, especially when the design solution is highly sensitive to probable uncertainties [1]. For example, it is usually difficult for deterministic approaches to satisfy these conventional design requirements: transonic free-shock or weak-shock design over a range of flight conditions, a wide spread low-drag design of natural-laminar-flow (NLF)[2] or robust rotor blade design under both manufacturing error and operating condition uncertainties. Therefore, with great advance in computer power and engineering refinement, demands for designers are ever increasing by incorporating uncertainty into system design and analysis to yield an economically viable solution at a minimum of cost and risk. Uncertainty-based design optimization (UBDO) , as a particularly promising methodology for this purpose, has been extensively recognized and utilized in many domains, e.g., aerodynamic shape optimization (ASO) [3-6], structure design undergoing fluid-structure interaction phenomena [7], etc. Unlike conventional optimization, UBDO involves a typically nested-loop optimization process, i.e.,

outer optimization loop and inner uncertainty quantification (UQ) loop. In outer loop, robust optimization executes Pareto-optimal solutions. This is usually a complex multi-objective optimization and trade-off problem, always involving typical conflicting objectives, i.e., enhancing the robustness of objective, improving the performance of objective, maintaining the reliability of design [8]. At each iteration point of outer optimization loop, it calls the UQ loop to perform both moment propagation and probability analysis of quantity of interest (QoI). In fact, the simulation models are often computationally expensive especially for complex vehicle design, e.g., Computational Fluid Dynamics (CFD) for aerodynamic analysis, Finite Element Analysis (FEA) for structure dynamic analysis [7], etc. As a result, the solution of an UBDO problem will draw in UQ of QoI and its integration within an optimization routine. Consequently, significant higher order of computational effort is associated with UBDO, as compared to the deterministic optimization.

To alleviate this issue, more studies revolve around the extensive development of efficient UQ techniques, e.g., polynomial chaos expansion (PCE)/sparse PCE [9, 10], stochastic collocation [11], Gauss-type integration [12] and sparse grid regulations [13], univariate/generalized dimension‐reduction method [14], Taylor series expansion-based method [15], universal Kriging or Co-Kriging method [3], etc. A recent review [5] has summarized these popular UQ methods and their characteristics. Among them, non-intrusive PCE (NIPCE) has revealed great potential and has attracted many designers to integrate it into UBDO process [4, 16, 17] since NIPCE can provide particularly efficient UQ with a comparable accuracy with respect to (w.r.t.) Monte Carlo simulation (MCS) technique. The charm of PCE lies on its mathematically rigorous concept, the mutual orthogonality of PC bases and good convergence for a general square-integrable stochastic process [18]. The establishment of PCE usually depends on two ways, i.e., Galerkin projection (GPNIPC) and point collocation (PCNIPC) methods. Although both methods show various advantages and disadvantages, with more random variables (RVs) and high-order response considered recently, they both suffer from the so-called *curse of dimensionality*. This motivates researchers to develop efficient methods for recovering the coefficients of NIPCE by reducing the size of stochastic problems, e.g., reduced-basis approach [19], adaptive basis approach [20], sparse basis [9, 21]. Recently, sparse approaches by ℓ_1 -minimization or weighted/ gradient-enhanced/ Multi-fidelity ℓ_1 -minimization algorithms [22-25] have been shown to be very efficient to reduce the computational cost of high-dimensional and high-order PCE when the solution (PCE coefficients) is sparse.

Forward selection algorithms, e.g. classical Least angle regressions (LAR) [26], select the significant basis at each step to aggressively reduce the squared error. However, they cannot correct mistakes made in earlier steps. Forward selection algorithms can early select certain basis which has the less contribution to the output when more significant bases are incorporated. Hence, this basis should be removed later to enhance sparsity and to improve prediction accuracy. Conversely, backward greedy algorithms can remove the basis from the candidate bases with the smallest increase of squared error. However, backward greedy algorithms probably overfit the data, which fail if all bases are removed and cannot effectively eliminate bad features, meanwhile with more computational cost. Hence, backward greedy algorithms need to start with a good candidate set that does not completely overfit the data. In other words, it can only correct errors with a small amount of overfitting.

In author's previous paper[27], we proposed a novel and efficient adaptive forward-backward selection (AFBS) technique for the sparse PC reconstruction. The AFBS technique combines the strength of both forward and backward selection algorithms while avoiding their shortcomings. AFBS technique iteratively and alternatively performs stepwise regression of forward and adaptive backward steps until the most significant bases are retained and all redundant or insignificant bases are discarded. This procedure is provably robust and efficient by fixing the drawbacks of forward selection algorithms, which is further validated by using many complex analytical functions and multiple challenging engineering applications. Some in-depth and comprehensive comparisons were also made with LAR and classical full PC methods. In this paper, we proposed a fully adaptive forward-backward selection (FAFBS) method for an adaptive construction of the optimal sparse PC representation. The remainder of the paper is organized as follows. The details of PC representations and available solving approaches of constructing PC representations are presented in Section 2 and 3. Next, in Section 4, a advised FAFBS algorithm and the complete procedure of FAFBS methodology are proposed. Then, an analytical function and an aerodynamic analysis problem for validating the effectiveness of proposed algorithm are illustrated in Section 5. Finally, some important conclusions are proposed in Section 6.

2. Polynomial Chaos Expansion

PC representations have been widely used for accurate representation of any square-integrable stochastic process or RV on a probability space (Ω, Θ, P), where Ω is a sample space, Θ is an appropriate σ-algebra on Ω and P is a probability measure on (Ω, Θ). Cameron-Martin [18] proved the convergence of the Wiener-Hermite PCE with Gaussian inputs for any $L^2(\Omega, \Theta, P)$ functional in the $L^2(\Omega, \Theta, P)$ sense. In case of more general distributions of inputs, Xiu and Karniadakis [10] have developed Generalized polynomial chaos (GPC) expansions by using a broader class of orthogonal polynomials in the Askey scheme, and illustrated that the Wiener-Askey PC exhibits exponential convergence. Each family of orthogonal polynomials corresponds to a given choice of distribution for the inputs. These orthogonal polynomials of different orders make up the complete bases in the random space. The convergence properties of different bases, and thus the number of bases required for a given accuracy, depend both on the approximated process/response and on the distribution of involved inputs. Therefore, it would be very promising if PCE employs Legendre polynomials for surrogating the design space due to the bounded and uniform search domain of engineering optimization problems. Reference [28] examined the performance of Legendre-PC-Kriging metamodel and other variants of universal Kriging methods applied in global optimization problems, and found that the Legendre-PC-Kriging metamodel is the best one considering the more robust performance compared with others. More importantly, when practical optimization problems inevitably involve uncertainties into the process, Legendre-PC representations are the most appropriate to approximate the stochastic response in terms of simultaneous inputs of design variables (DVs) and random variables (RVs). In addition, the statistical moments of stochastic response at each candidate design can be estimated cheaply by PC-Kriging metamodel based on MCS technique.

Let $f \in L^2(\Omega)$ denote a real valued random variable, i.e., $f: \Omega \to \mathrm{R}$, which can be represented as

$$f(\mathbf{X}) = a_0\Gamma_0 + \sum_{i_1=1}^{\infty} a_{i_1}\Gamma_1(x_{i_1}) + \sum_{i_1=1}^{\infty}\sum_{i_2=1}^{i_1} a_{i_1,i_2}\Gamma_2(x_{i_1}, x_{i_2}) + \cdots, \tag{1}$$

where Γ_k denotes the Legendre polynomial of order k in terms of the input vector $(x_1, x_2, \cdots x_n)$. The d and n represent the dimensionality of DVs $\mathbf{X}$ and RVs Ξ involved in the design system, respectively. The $\mathbf{X} = (x_1, x_2, \cdots x_n)$ comprises the vector $(x_1, x_2, \cdots x_n)$ where $\mathbf{X} = (x_1, x_2, \cdots x_d)$ is defined as RV vector. In practical usage, we can always assume that the input vector $\mathbf{X}$ consists of n variables with independent, uniformly distributed entries. Further, the PCE can be rewritten succinctly as

$$f(\mathbf{X}) = \sum_{j=0}^{\infty} \beta_j \psi_j(\mathbf{X}), \tag{2}$$

where there is a one-to-one correspondence between the coefficients and functionals in Eq. (1) and those in Eq. (2). The multi-dimensional polynomials $\psi_j(\mathbf{X})$ are constructed by tensorizing univariate polynomials,

$$f(\mathbf{X}) = \sum_{j=0}^{\infty} \beta_j \psi_j(\mathbf{X}), \tag{3}$$

where $\{\psi_{k_i}(x_i)\}$ $(i = 1,2,\cdots,n)$ represents the complete set of orthonormal polynomials of degree k_i $(k_i = 0,1,\cdots,\infty)$ with respect to the probability density function $\rho_i(x_i)$. The $\psi_j(\mathbf{X})$ of total order p implies that we consider all polynomials satisfying

$$|\mathbf{k}| = \sum_{i=1}^{n} k_i \le p \qquad k_i = 0,1,\cdots,p. \tag{4}$$

where $\mathbf{k} = (k_1, k_2, \cdots, k_n)$. When the polynomial chaos is truncated at p polynomial order, $f(\mathbf{X})$ can be expressed as the summation of M_p PC terms

$$f(\mathbf{X}_\Xi) = \sum_{i=1}^{M_p} \beta_i \psi_i(\mathbf{X}) + \varepsilon(\mathbf{X}), \tag{5}$$

where ε is the truncation error and $M_p = (p+n)!/p!\,n!$. The PC expansions form the complete orthogonal bases in the $L^2(\Omega, \Theta, P)$ space of the homologous inputs, i.e.,

$$\langle \psi_i, \psi_j \rangle = \langle \psi_i^2 \rangle \delta_{ij}, \tag{6}$$

where δ_{ij} is Kronecker delta and $\langle \cdot, \cdot \rangle$ denotes the ensemble average. For given truncation error, the

procedure of constructing PC representations is to efficiently and accurately estimate PC coefficients. There exist two popular solution approaches, i.e., GPNIPC and PCNIPC. In this paper, the PCNIPC is used for calculating the PC coefficients. The PCNIPC applies a regression technique in the L_2 sense to obtain the polynomial coefficients by solving an over-determined least squares problem, which is given by

$$\boldsymbol{\beta} = \left(\boldsymbol{\Psi}^T\boldsymbol{\Psi}\right)^{-1}\boldsymbol{\Psi}^T\mathbf{Y}, \tag{7}$$

where $\boldsymbol{\Psi} = \{\psi_i(\mathbf{X}^{(j)})\}_{N\times M_p} = [\boldsymbol{\psi}_1, \boldsymbol{\psi}_2, \cdots, \boldsymbol{\psi}_{M_p}]$ represents the measurement matrix. The each column $\boldsymbol{\psi}_i$ of $\boldsymbol{\Psi}$ is computed by substituting N observed points $\{\mathbf{X}^{(j)}\}_{j=1}^N$ into candidate PC basis $\psi_i(\mathbf{X})(i = 1,2,\cdots,M_p)$. $\mathbf{Y} = (f(\mathbf{X}^{(1)}), f(\mathbf{X}^{(2)}), \cdots, f(\mathbf{X}^{(N)}))^{\mathrm{T}}$ contains the N realizations of $f(\mathbf{X})$ from the observed points $\{\mathbf{X}^{(j)}\}_{j=1}^N$. The $\boldsymbol{\beta} = (\beta_1, \beta_2, \cdots, \beta_{M_p})^{\mathrm{T}}$ denotes the column vector of PC coefficients. As a necessary condition, $N \geq M_p$ is required to achieve a stable approximation of $\boldsymbol{\beta}$. The number of PC terms grows exponentially with both the dimension of inputs and PC order. As a result, using full PC representations rapidly becomes unaffordable as the dimension of inputs increases. To circumvent this issue, building sparse PC representations by ℓ_1-minimization or some efficient basis adaptive selection algorithms has extensively been researched when the solution (PCE coefficients) is sparse.

3. Sparse polynomial chaos via ℓ_1-minimization

When PC coefficients $\boldsymbol{\beta}$ are sparse, we seek to identify the small cardinality κ of $\boldsymbol{C} = \{\beta_i | \beta_i \neq 0\}$, and so look to efficient techniques from the field of compressed sensing or ℓ_0-minimization. However, ℓ_0-minimization generally suffers from the high computational cost due to the exponential number for candidate PC terms. To circumvent an exponential dependence, the convex relaxation of ℓ_0-regularization based on ℓ_1-minimization [29], also referred to as basis pursuit denoising or compressing sensing[30], has been developed, as given by

$$\min_{\boldsymbol{\beta}} \|\boldsymbol{\beta}\|_1, \ \ s.t. \left\|\boldsymbol{\Psi}\boldsymbol{\beta} - \mathbf{Y}\right\|_2^2 \leq \varepsilon, \tag{8}$$

where $\|\boldsymbol{\beta}\|_1$ denotes the ℓ_1 norm of $\boldsymbol{\beta}$, and ε is a tolerance of solution inaccuracy due to the truncation of the expansion. $\boldsymbol{\Psi}$ needs to satisfy certain conditions [31] to guarantee that the solution $\boldsymbol{\beta}$ by ℓ_1-minimization is the same or approximate with that by ℓ_0-minimization, e.g., the restricted isometry property (RIP) [32]. Some studies [29, 33] have demonstrated that the Legendre matrix is able to meet the strict requirements of RIP for ℓ_1-minimization regularization. Therefore, sparse PCE reconstruction by Eq. (8) has been researched and developed using many efficient algorithms. These algorithms include basis pursuit and greedy algorithms (the reader may refer to [27, 34] for more details), e.g., orthogonal matching pursuit (OMP) and least angle regressions (LAR) are the widely used greedy algorithms.

In this paper, we focus the novel adaptive forward-backward selection (FAFBS) method[27]. The detailed procedure of AFBS algorithm is presented in [27]. The AFBS technique combines the strength of both forward and backward selection algorithms while avoiding their shortcomings. AFBS technique iteratively and alternatively performs stepwise regression of forward and adaptive backward steps until the most significant bases are retained and all redundant or insignificant bases are discarded. The algorithm starts with an empty active set $A'^{(0)} = \phi$ which contains no basis vector at the iteration step $k = 0$. The next step $(k = k + 1)$ after initialization is a first forward selection step. The forward selection algorithm can refer to OMP. The most correlated basis $\boldsymbol{\psi}_{i^\circ}$ is first selected and is added to the current active set $A'^{(k)}$. The prediction vector $\boldsymbol{\mu}^{(k)}$ is updated by

$$\boldsymbol{\mu}^{(k)} = \boldsymbol{\psi}_{i^\circ}\left((\boldsymbol{\psi}_{i^\circ})^{\mathrm{T}}\boldsymbol{\psi}_{i^\circ}\right)^{-1}(\boldsymbol{\psi}_{i^\circ})^{\mathrm{T}}\mathbf{Y}. \tag{9}$$

Then, the adaptive forward-backward selection procedure is performed $(k = k + 1)$. The first selection step is the forward selection step by OMP algorithm. After the significant predictor $\boldsymbol{\psi}_{i^*}$ is selected from forward selection criterion, the current active set $A'^{(k)}$, the cumulative decrease of squared error d^+ and the cumulative change of squared error d are updated, namely $A'^{(k)} = A'^{(k-1)} \cup \{\boldsymbol{\psi}_{i^*}\}$, $d^+ = d^+ + \delta^+$, and $d = d + \delta^+$, where the decrease of squared error δ^+ at each iteration k is given by

$$\delta^+ = \frac{1}{N}\left(\left\|\mathbf{Y} - \boldsymbol{\mu}^{(k-1)}\right\|_2^2 - \left\|\mathbf{Y} - \boldsymbol{\mu}^{(k)}\right\|_2^2\right), \tag{10}$$

and the prediction vector $\boldsymbol{\mu}^{(k)}$ is also updated by

$$\boldsymbol{\mu}^{(k)} = \boldsymbol{\Psi}_{A^{(k)}} \hat{\boldsymbol{\beta}}^{(k)}, \tag{11}$$

where $\boldsymbol{\Psi}_{A'(k)}$ represents the current active basis vector matrix, i.e., $\boldsymbol{\psi}_i \in A'^{(k)}$ is the column vector of $\boldsymbol{\Psi}_{A'(k)}$ in order. The $\widehat{\boldsymbol{\beta}}^{(k)}$ is estimated by

$$\hat{\boldsymbol{\beta}}^{(k)} = \arg\min_{\hat{\boldsymbol{\beta}}} \left\| \mathbf{Y} - \boldsymbol{\Psi}_{A^{(k)}} \hat{\boldsymbol{\beta}} \right\|_2 = ((\boldsymbol{\Psi}_{A^{(k)}})^{\mathrm{T}} \boldsymbol{\Psi}_{A^{(k)}})^{-1} (\boldsymbol{\Psi}_{A^{(k)}})^{\mathrm{T}} \mathbf{Y}. \tag{12}$$

When no less than two predictors have been added to active set $A'^{(k)}$, backward selection algorithm is carried out automatically. The backward selection algorithm will remove the insignificant or redundant predictors. The insignificant basis vectors are those that the least squares loss slightly increases or δ^- near zero when they are removed from the current active set. The backward selection step selects the insignificant predictor by the criterion

$$i^{\#} = \arg\min_i \frac{\left| \boldsymbol{\psi}_i^T (\mathbf{Y} - \boldsymbol{\Psi}_{A^{(k)} - \{\boldsymbol{\psi}_i\}} \hat{\boldsymbol{\beta}}_{i^-}^{(k)}) \right|}{\left\| \boldsymbol{\psi}_i \right\|_2}, \tag{13}$$

where $\widehat{\boldsymbol{\beta}}_{i^-}^{(k)}$ represents the coefficients estimates of basis vectors in current active set $A'^{(k)}$ without the basis vector $\boldsymbol{\psi}_i$, as given by

$$\hat{\boldsymbol{\beta}}_{i^-}^{(k)} = \arg\min_{\hat{\boldsymbol{\beta}}} \left\| Y - \boldsymbol{\Psi}_{A^{(k)} - \{\boldsymbol{\psi}_i\}} \hat{\boldsymbol{\beta}} \right\|_2 = ((\boldsymbol{\Psi}_{A^{(k)} - \{\boldsymbol{\psi}_i\}})^{\mathrm{T}} \boldsymbol{\Psi}_{A^{(k)} - \{\boldsymbol{\psi}_i\}})^{-1} (\boldsymbol{\Psi}_{A^{(k)} - \{\boldsymbol{\psi}_i\}})^{\mathrm{T}} \mathbf{Y}, \tag{14}$$

wherein $\boldsymbol{\Psi}_{A'(k) - \{\boldsymbol{\psi}_i\}}$ denotes the remaining active basis vector matrix when removing $\boldsymbol{\psi}_i$ from the current active set $A'^{(k)}$. In addition, the backward selection criterion can also be applied to select the insignificant basis vector as

$$i^{\#} = \arg\min_i \left\| Y - \mathbf{Y} - \boldsymbol{\Psi}_{A^{(k)} - \{\boldsymbol{\psi}_i\}} \hat{\boldsymbol{\beta}}_{-i}^{(k)} \right\|_2, \tag{15}$$

where $\boldsymbol{\psi}_i \in A'^{(k)}$, and $\widehat{\boldsymbol{\beta}}_{-i}^{(k)}$ denotes the remaining vector when removing the coefficients of $\boldsymbol{\psi}_i$ from coefficients estimates vector $\widehat{\boldsymbol{\beta}}^{(k)}$ calculated by Eq. (12). The two backward selection criteria show a slight difference. In terms of the three applications presented in later sections, our proposed criterion (Eq. (13)) provides a better performance.

After the candidate predictor $\boldsymbol{\psi}_{i^{\#}}$ is selected, we decide whether $\boldsymbol{\psi}_{i^{\#}}$ can be removed. The increase of least squares loss namely δ^- is first estimated by

$$\delta^- = \frac{1}{N} \left(\left\| \mathbf{Y} - \bar{\boldsymbol{\mu}} \right\|_2^2 - \left\| \mathbf{Y} - \boldsymbol{\mu}^{(k)} \right\|_2^2 \right), \tag{16}$$

where $\bar{\boldsymbol{\mu}}$ is defined as prediction vector of output vector by subtracting the contribution of $\boldsymbol{\psi}_{i^{\#}}$ namely

$$\bar{\boldsymbol{\mu}} = \boldsymbol{\Psi}_{A^{(k)} - \{\boldsymbol{\psi}_{i^{\#}}\}} \hat{\boldsymbol{\beta}}_{i^{\#-}}^{(k)}, \tag{17}$$

wherein $\widehat{\boldsymbol{\beta}}_{i^{\#-}}^{(k)}$ represents the coefficients estimates of basis vectors in current active set $A'^{(k)}$ without the basis vector $\boldsymbol{\psi}_{i^{\#}}$, as given by

$$\hat{\boldsymbol{\beta}}_{i^{\#-}}^{(k)} = \arg\min_{\hat{\boldsymbol{\beta}}} \left\| \mathbf{Y} - \boldsymbol{\Psi}_{A^{(k)} - \{\boldsymbol{\psi}_{i^{\#}}\}} \hat{\boldsymbol{\beta}} \right\|_2 = ((\boldsymbol{\Psi}_{A^{(k)} - \{\boldsymbol{\psi}_{i^{\#}}\}})^{\mathrm{T}} \boldsymbol{\Psi}_{A^{(k)} - \{\boldsymbol{\psi}_{i^{\#}}\}})^{-1} (\boldsymbol{\Psi}_{A^{(k)} - \{\boldsymbol{\psi}_{i^{\#}}\}})^{\mathrm{T}} \mathbf{Y}. \tag{18}$$

The threshold parameter v_1 is selected by designers to remove the insignificant predictor $\boldsymbol{\psi}_{i^{\#}}$ when the cumulative increase change of squared error d^- is smaller than the threshold value $v_1 d^+$. Here d^- is estimated as $d^- = d^- + \delta^-$. When $\boldsymbol{\psi}_{i^{\#}}$ can be removed from the current active set, the prediction vector of output is updated by

$$\boldsymbol{\mu}^{(k)} = \bar{\boldsymbol{\mu}}, \tag{19}$$

and the cumulative change of squared error namely d is also updated by $d = d + \delta^-$. Otherwise, the accumulative increase d^- of least squares loss should be corrected to subtract the significant increase of δ^-, i.e., $d^- = d^- - \delta^-$. The adaptive forward-backward selection step should be stopped once the stopping criterion is satisfied or the universal set Σ' is traversed. The stopping criterion means that the prediction residual error $\left\| \mathbf{Y} - \boldsymbol{\mu}^{(k)} \right\|_2$ is less than the specified criterion ϵ. After reaching the stopping criterion, a first set of significant predictors is derived. Then, it is noticed that a backward checking step is appended after the adaptive forward-backward selection step. The purpose of this step is to check all predictors in the active set again. We will remove the insignificant predictor $\boldsymbol{\psi}_{i^{\#}}$ from current active set $A'^{(k)}$ when the increase of least squares loss δ^- is less than $v_2 d$,

i.e., $\delta^- < v_2 d$. The definitions of δ^- and $\bar{\boldsymbol{\mu}}$ are the same as in Eq. (16) and Eq. (17). δ^- and $\bar{\boldsymbol{\mu}}$ are updated when the $\boldsymbol{\psi}_{i^\#}$ is removed. The procedure of backward checking step is similar with the backward selection step. The detailed procedure is showed in Figure 1.

As a contrast, the forward selection algorithms all share the basic regulation of greedily picking an additional predictor at each step to aggressively reduce the squared error. However, a major flaw of forward selection algorithms is that it cannot correct mistakes made in earlier steps. For example, OMP algorithm is utilized to select the most relevant sparse set of polynomials for building up the PC metamodel. OMP starts from initial active set $A^{(0)} = \phi$ and initial residual vector $\boldsymbol{\gamma}^{(0)} = \mathbf{Y}$. At each iteration k, OMP identifies only the most correlated basis with the current residual $\boldsymbol{\gamma}^{(k)}$. The residual vector $\boldsymbol{\gamma}^{(k+1)}$ is updated by subtracting the contribution of selected bases in active set from the output vector. The iteration procedure is continued until the residual tolerance ε is achieved. On the other hand, backward greedy algorithms consecutively remove one insignificant basis vector (with the smallest contribution or no contribution to the output) from the universal set Σ at each iteration. However, as backward greedy algorithm starts with universal set Σ, it is more time-consuming, namely $N \gg M$. In addition, the method often causes over-fitting when $M \gg N$, namely any basis function cannot be removed from Σ. Therefore, backward greedy algorithm needs to start with a good model that contains errors with a small amount of insignificant or redundant basis functions [35]. Therefore, the proposed novel adaptive forward-backward selection (AFBS) algorithm shows significant advantages over other greedy algorithms.

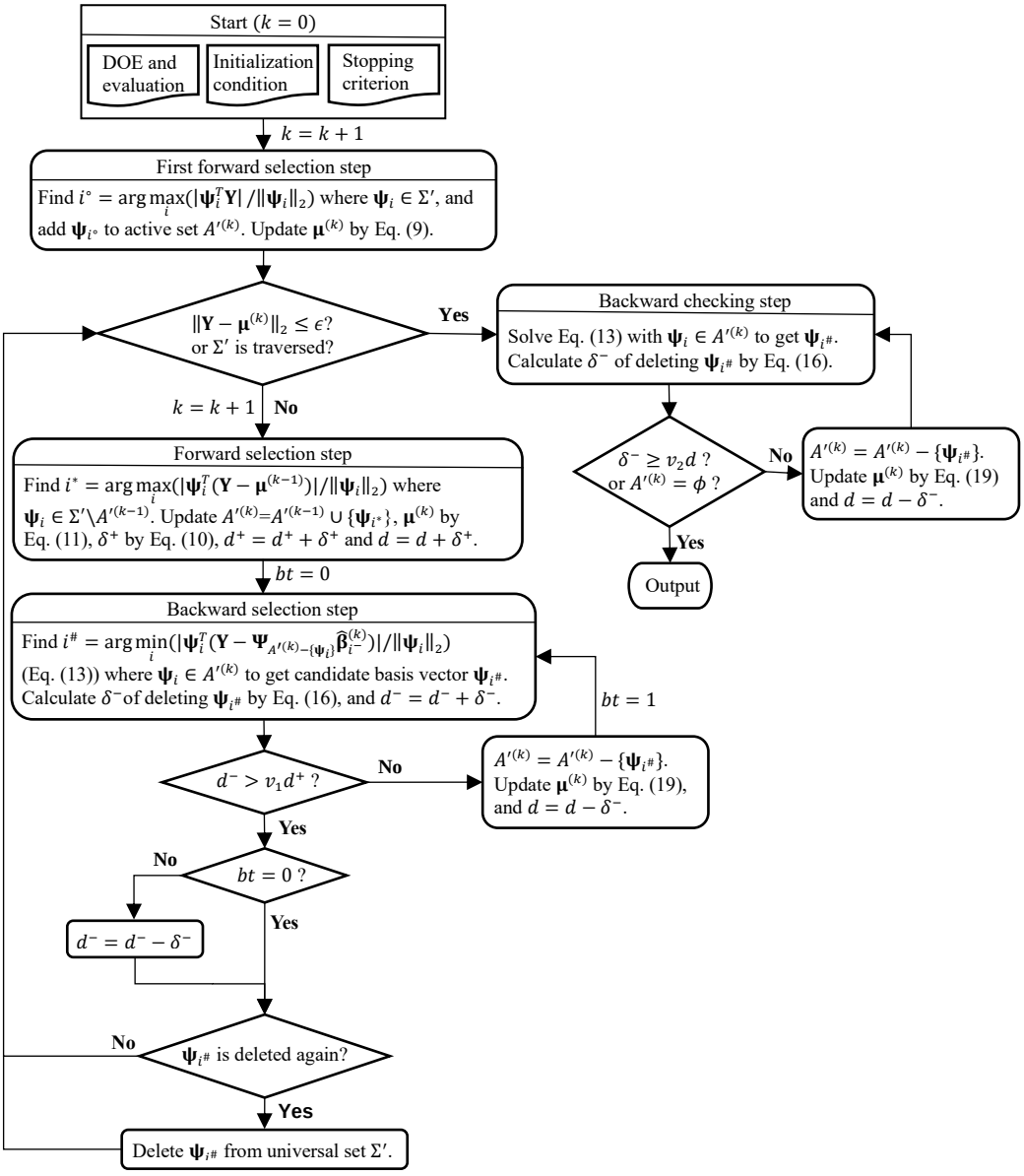

Figure 1 Flowchart of AFBS algorithm

4. Fully adaptive forward-backward selection (FAFBS) method

The original AFBS algorithm was first proposed in [27]. However, as presented in the AFBS algorithm, the sparsity of the final PC representations obtained by the AFBS method is related to the choice of the two threshold parameters. The appropriate values of the two threshold parameters can obtain a slightly better PC metamodel. Therefore, in this paper a fully adaptive forward-backward selection (FAFBS) algorithm is proposed by involving an efficient optimization search algorithm for selecting the optimal values for the two threshold parameters. To obtain the optimal sparse PC metamodel and to make the reconstructing procedure more convenient for users, a fully adaptive forward-backward selection (FAFBS) method is proposed in this paper. As shown in Figure 2, the novel method improves the original AFBS algorithm by involving an optimization search process with minimizing the cross-validation error. Compared with the original AFBS algorithm, the novel method is fully adaptive and recovers the most important PC coefficients with the adaptive selection of the two threshold parameters.

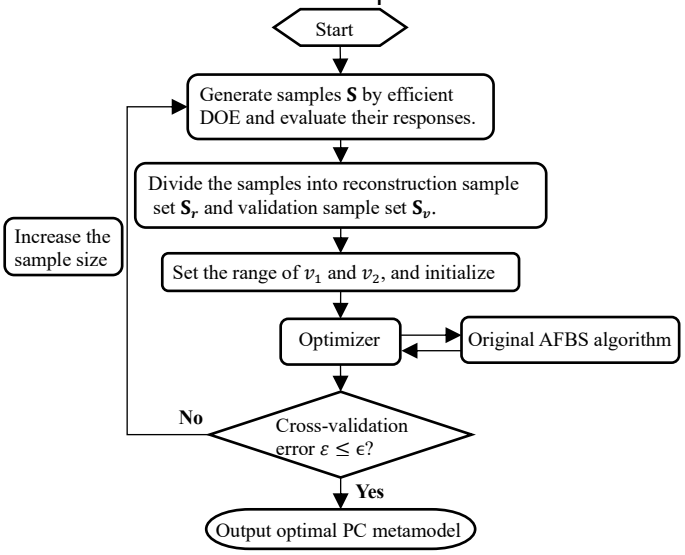

Figure 2 FAFBS algorithm for building the optimal sparse PC metamodel

5. Application to numerical examples and aerodynamic problems

In this section, two representative cases are dedicated to systematically examine the performance of the proposed FAFBS technique. The developed method is first applied to the four-dimensional Park function. Then, an aerodynamic problem with high-dimensional RVs is minutely considered to further assess the applicability and efficiency of the developed method. The case involves the transonic flow over the RAE2822 airfoil with combined geometrical and operational uncertainties. The results are presented in detail and compared with those by OMP algorithm and full PC method.

5.1 Numerical examples

The four-dimensional Park function[36] is defined as

$$y(\mathbf{X}) = \frac{x_1}{2}\left[\sqrt{1+(x_2+x_3^2)\frac{x_4}{x_1^2}}-1\right]+(x_1+3x_4)\exp\left[1+\sin(x_3)\right],\ x_i \in U[0,1] \tag{20}$$

where x_1, x_2, x_3, x_4 are assumed to be uniformly distributed. Park function is widely used for benchmarking in uncertainty quantification and sensitivity analysis. The reference statistical moments are estimated using Monte Carlo Simulation (MCS) with 1×10^6 Latin hypercube points being used. A PC degree of $p = 9$ is used by the developed FAFBS, OMP and full PC methods to build the PC approximation for the Park function. The convergence comparison of relative errors in standard deviation (σ_y) and mean (μ_y) of Park function with the increasing number of samples is shown in Figure 3. The developed method, with $v_1 = 0.1, v_1 = 0.005$, obtains the obvious fastest convergence rate of error and the best approximation accuracy for quantity of interest (QoI), thus for a given error it requires the far least number of model evaluations, compared to OMP and full PC methods. It can be also found that the two sparse optimization approaches for reconstructing PC significantly perform better than full PC method which shows the slowest convergence rate of error. For example, when given $N = 70$ samples, the FAFBS method achieves the relative errors in σ_y and μ_y as 0.0696 and 0.0190, respectively, while OMP method gets the corresponding errors of 0.4624

and 0.5871 separately. Table 1 gives some detailed results obtained by the three methods. Results demonstrate that the developed FAFBS approach obtains a sparser solution and significantly outperforms than OMP and full methods.

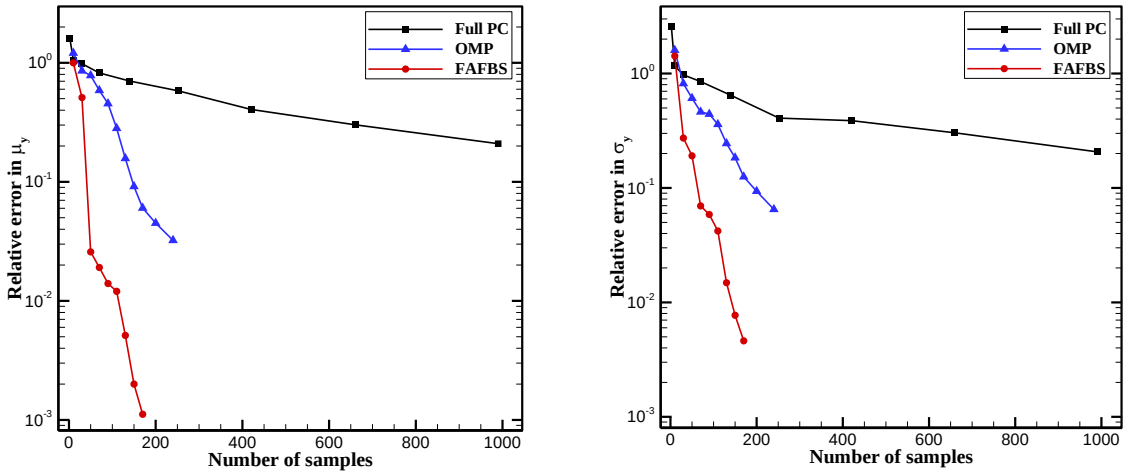

Relative error in mean (μ_y) Relative error in standard deviation (σ_y)

Figure 3 Comparison of variation of relative errors in mean (left) and standard deviation (right) of Park function using FAFBS, OMP, and Full PC methods.

Table 1 Comparison of statistical moments obtained using full PC, OMP and AFBS methods

Methods	Sample size	Card (A)	Relative error	
			$e(\mu_y)$	$e(\sigma_y)$
Full PC	990	495	0.2093	0.2068
OMP	200	42	0.0451	0.0937
FAFBS	170	12	0.0011	0.0046

5.2 Transonic RAE2822 airfoil

The case of the transonic flow over the RAE2822 airfoil is often used for benchmarking uncertainty analysis and optimization techniques [24, 26]. It has been widely acknowledged that the complex flow field about any of the designed airfoils is sensitive to just about everything [37-40]. This includes the flow conditions, geometry error, turbulence model, grid, etc. Such phenomena often lead to the ill posed deterministic aerodynamic optimization. In extreme cases, it can yield designs with very undesirable aerodynamic characteristics occurring at off-design, and even on-design. The off-design nominal flow conditions considered here correspond to a freestream Mach number (Ma) of 0.734, a lift coefficient (C_l) of 0.824 (or angle of attack of $\alpha = 2.79^o$), and a Reynolds number (Re) of 6.5×10^6. Therefore, the case considering the performance uncertainty is very meaningful for resolving the abovementioned issue and very challenging for examining the uncertainty analysis and uncertainty-based design optimization technique[5, 16, 41].

In this present study we consider inevitable uncertainties arising from the nominal flow conditions and the nominal CAD model [42]. The Mach number and angle of attack are considered as RVs imposed on practical operational conditions ($Ma = 0.734, \alpha = 2.79^o, Re = 6.5 \times 10^6$). They are assumed to be uniformly distributed, i.e., $Ma = \mu_M + \xi_M \sigma_M$, and $\alpha = \mu_\alpha + \xi_\alpha \sigma_\alpha$, where $\mu_M = 0.734, \sigma_M = 0.01, \mu_\alpha = 2.79^o, \sigma_\alpha = 0.2^o$, and $\xi_M, \xi_\alpha \sim U(-1,1)$. Because of manufacturing variations, no real aerodynamic shape exactly conforms to its nominal geometry. As a result, the manufactured mean is clearly different from the nominal CAD design intent. The cost of manufacturing is assumed to increase as the tolerance scheme is stricter, i.e. less geometric variability is allowed. Therefore, geometrical uncertainty resulting from manufacturing error and geometry deformation should be considered to impose manufacturing tolerance.

Geometrical uncertainty is modelled as a RV $e(s,\omega)$ where s indexes the spatial location on the geometry surface and ω indexes the probability space. The RV $e(s,\omega)$ describes the error between the manufactured surface and the nominal (design intent) CAD surface in the normal direction. The manufactured geometry surface can be given as

$$X(s,\omega) = \bar{X}(s) + e(s,\omega)\vec{n}(s) \qquad \forall s \in S, \tag{21}$$

where $\vec{n}(s)$ is the unit vector in s normal to the profile S. $\bar{X}(s)$ is normal surface. The error function is uniquely defined by random variable $e(s,\omega)$ with mean $\bar{e}(s,\omega)$ and exponential covariance function $R(s_1,s_2)$. The covariance function $R(s_1,s_2)$ describes the smoothness and correlation length of the random variable, as given by

$$R(s_1,s_2)=\sigma^2 e^{-|s_1-s_2|/l}, \tag{22}$$

where σ is forced to be positive everywhere, since a zero $\sigma(s_0)$ implies no geometric variability at s_0. For simplicity, the σ is constant with a variation of s. The variables s_1 and s_2 are positions along the airfoil, with $s=0$ at the trailing edge, increase along the lower surface toward the leading edge and along the upper surface from leading edge toward the trailing edge. In this case, for initial geometry (RAE 2822 airfoil), the maximum value of s is 2.032, i.e., $0 \le s \le 2.032$.

The Karhunen–Loève (K-L) expansion is applied to model the random variable $e(s,\omega)$.

$$e(s,\omega)=\bar{e}(s)+\sum_{i=1}^{\infty}\sqrt{\lambda_i}\phi_i(s)\xi_i(\omega), \tag{23}$$

where $\xi_i(\omega)$ are uncorrelated random variables. The mean $\bar{e}(s)$ is assumed to be zero everywhere, and the λ_i and ϕ_i are the eigenvalues and eigenfunctions of the covariance kernel, respectively. The eigenfunctions problem and eigenvalues have analytical solution for such kind of kernel function [43]. The order of truncation K is chosen so that the truncated series retain the most of the energy of the original random process, i.e.,

$$\sum_{i=1}^{K}\lambda_i \Big/ \sum_{i=1}^{\infty}\lambda_i \ge 0.90. \tag{24}$$

According present analysis, when correlation length l reaches the value of 0.2, the decay rate of eigenvalues is mild. In addition, the mode frequency of the eigenfunctions $\phi_i(s)$ increases with the increase in index i. Combined with Eq. (24), we use a truncated K-L expansion with finite terms to represent the RV $e(s,\omega)$. Figure 4 illustrates the 30 different random realizations of RAE2822 airfoil shape for $\sigma=0.0015$ and $l=0.2$. Figure 5 shows the computed pressure coefficients distributions of the 30 random airfoils. A larger σ will lead to a larger discrepancy of practical shape relative to the nominal intent value and larger deviation of pressure distributions from the deterministic values. Considering the largely improvement of manufacturing level, we choose $l=0.2,\sigma=0.0015$ for assessing the effect of geometrical uncertainty. It is noted that in order to avoid the intersection at the trailing edge of these stochastic airfoils, the standard deviation σ at the trailing edge is appropriately reduced. Further, the first 12 eigenvalues and eigenfunctions are utilized in the truncated K-L expansion, which implies that 12 random variables are used to define the geometrical uncertainty. They are assumed to be uniformly distributed, i.e., $\xi_i \sim U(-1,1), i=1,2,\cdots,12$. Therefore, considering the operational and geometrical uncertainties simultaneously, a total of 14 RVs ($\Xi=(\xi_M,\xi_\alpha,\xi_1,\xi_2,\cdots\xi_{12})$) are considered on high-dimensional stochastic space $[-1,1]^{14}$ for this present analysis.

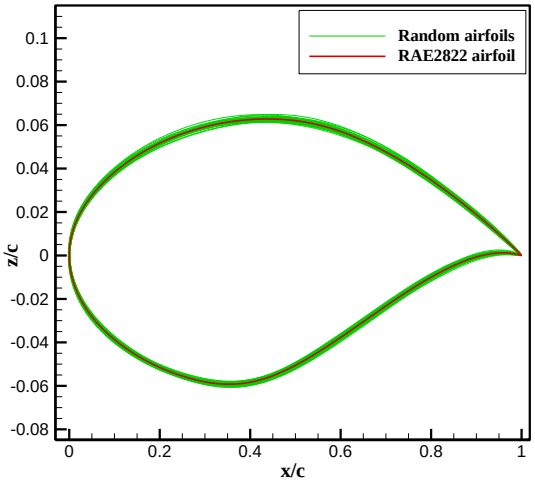

Figure 4. 30 random realizations of RAE2822 airfoil shape ($l=0.2,\sigma=0.0015$)

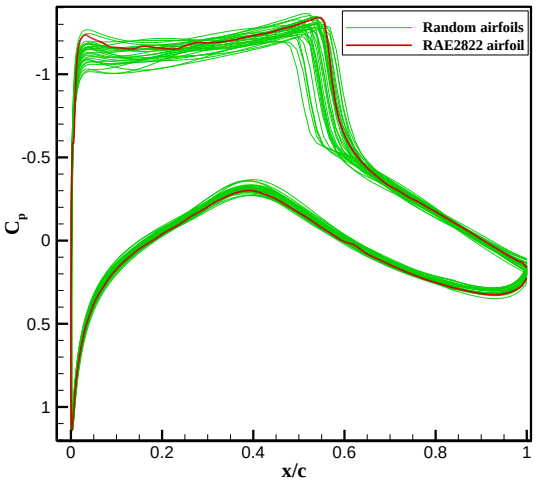

Figure 5. Pressure coefficients distributions of 30 random realizations of RAE2822 airfoil shape ($l=0.2,\sigma=0.0015$).

Next, the proposed AFBS algorithm is used to reconstruct the sparse PC representations of stochastic

performance of RAE2822 airfoil. As a contrast, OMP algorithm and full PC are also utilized to build PC metamodel. The reference statistical moments are calculated using MCS based on 10^4 LHS points, as shown in Table 2. Figure 6 gives the comparision of convergence of relative errors in mean (μ_{C_d})and standard deviation (σ_{C_d}) of drag coefficient using the three methods to reconstruct PC. Results reveal that the two sparse reconstruction methods show a faster convergence rate than full PC approach. More importantly, the developed method achieves the fastest convergence rate of error with increasing number of samples, and obtains the least relative error when given the same sample size. As shown in Table 2, given sample size $N = 190$, the AFBS method obtains the errors of μ_{C_d} and σ_{C_d} within 1 count (10^{-4}), while classic full PC and OMP methods get far larger errors of μ_{C_d} and σ_{C_d} than 3 counts even though they utilize more samples. The same findings can be reached in Figure 7, which shows the relative errors in mean μ_{C_l} and standard deviation μ_{C_l} of lift coefficient with increasing number of samples. It turns out that, for a specified accuracy of moments propagation, the developed method requires far less number of samples than full and OMP methods. Notably, The developed method selects the most significant PC terms and builds up sparser PC representations.

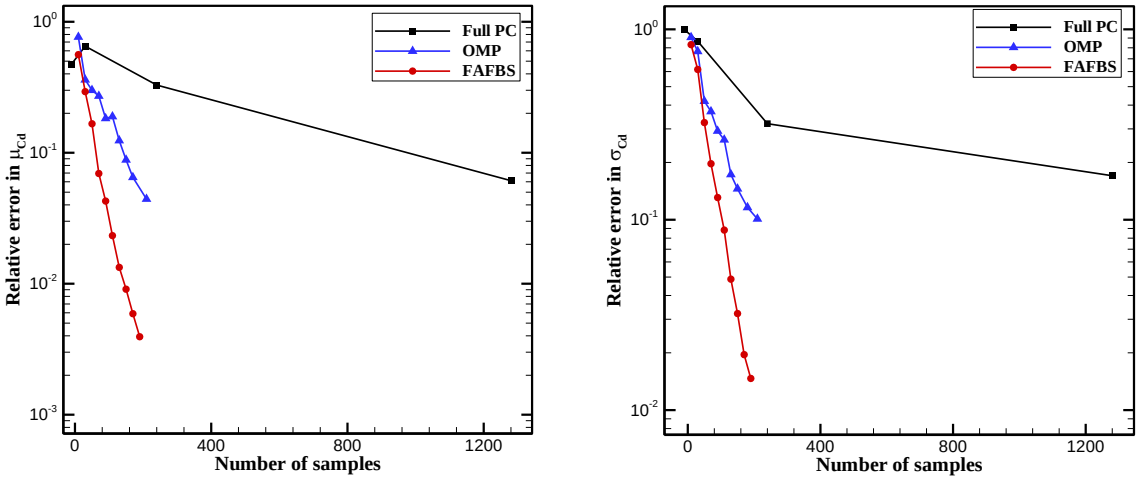

Figure 6 Variation of relative errors in $\boldsymbol{\mu_{C_d}}$**(left)** and $\boldsymbol{\sigma_{C_d}}$**(right)** obtained using the developed FAFBS method, compared to OMP and full PC methods.

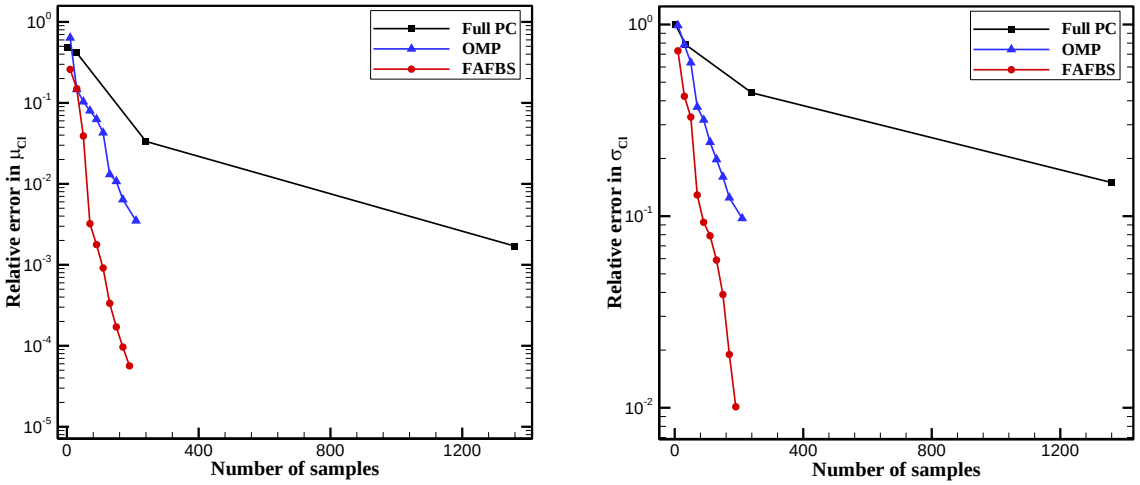

Figure 7 Variation of relative errors in $\boldsymbol{\mu_{C_l}}$**(left)** and $\boldsymbol{\sigma_{C_l}}$**(right)** obtained using the developed FAFBS method, compared to OMP and full PC methods.

Table 2 Comparison of relative errors obtained using full PC, OMP and AFBS methods

Methods	Sample size	Card (A)	$\mu_{C_d}, e(\mu_{C_d})$	$\sigma_{C_d}, e(\sigma_{C_d})$	$\mu_{C_l}, e(\mu_{C_l})$	$\sigma_{C_l}, e(\sigma_{C_l})$
MCS (reference)	1×10^4	--	0.018739	0.003161	0.798697	0.03055
Full PC	1360	680	0.061185	0.170190	0.001699	0.149724
OMP	210	29	0.044283	0.100995	0.003502	0.097362
FAFBS	**190**	**14**	**0.003936**	**0.014668**	**0.000056**	**0.010120**

6. Conclusion

In this paper, a novel fully adaptive forward-backward selection (FAFBS) algorithm is developed to reconstruct sparse PC efficiently and adaptively. The devised algorithm combines the strengths of both forward and backward selection algorithms and avoids their shortcomings. The algorithm starts by the forward selection step which adds significant PC terms to the candidate set, and is automatically followed by an adaptive backward elimination step which removes redundant candidate predictors step by step until all potential PC terms are detected. Compared to classical forward selection methods, e.g., LAR and OMP algorithms, the proposed algorithm tends to only capture the most significant PC contributions, so as to enhance sparsity and improve accuracy for PC approximation when given limited number of samples. The efficiency of the developed FAFBS algorithm is successfully validated in several challenging applications compared to OMP method. First, one complex analytical function with three normally distributed random variables is considered. An in-depth comparison considering the estimated error of moment propagation using the FAFBS technique, the OMP algorithm and the full PC is carried out. It indicates that the developed FAFBS algorithm builds a sparser and more accurate PC metamodel than other methods given the same number of samples. Furthermore, an challenging aerodynamic analysis case is utilized to thoroughly examine the performance of the proposed algorithm. It analyzes the aerodynamic performance of a transonic airfoil under operational and geometrical uncertainties. Detailed error analysis in moment estimation of $C_D$and $C_l$are compared. The results reveal the same trend, i.e., the FAFBS algorithm always needs the least number of samples than OMP and full PC for a specific estimate accuracy. Meantime, to achieve the same estimate accuracy, the OMP and full PC methods will require far more samples than FAFBS technique.

7. Contact Author Email Address

Corresponding author: Huan Zhao, zhaoh63@mail.sysu.edu.cn

8. Copyright Statement

References

[1] Zang, T. A., Hemsch, M. J., Hilburger, M. W., Kenny, S. P., Luckring, J. M., Maghami, P., Padula, S. L., and Stroud, W. J. "Needs and opportunities for uncertainty-based multidisciplinary design methods for aerospace vehicles," NASA/TM-2002-211462. NASA Langley Research Center, 2002.

[2] ZHAO, H., Gao, Z., and Xia, L. " Research on efficient robust aerodynamic design optimization method of high-speed and high-lift NLF airfoil," Acta Aeronautica et Astronautica Sinica Vol. 42, No. 7, 2021,1-18, 124894. doi: 10.7527/S1000-6893.2020.24894

[3] Keane, A. J. "Cokriging for robust design optimization," AIAA Journal Vol. 50, No. 11, 2012, pp. 2351-2364.

[4] Wang, X., Hirsch, C., Liu, Z., Kang, S., and Lacor, C. "Uncertainty‐based robust aerodynamic optimization of rotor blades," International Journal for Numerical Methods in Engineering Vol. 94, No. 2, 2013, pp. 111-127.

[5] Zhao, H., Gao, Z., Xu, F., and Zhang, Y. "Review of Robust Aerodynamic Design Optimization for Air Vehicles," Archives of Computational Methods in Engineering Vol. 26, No. 3, 2019, pp. 685-732. doi: 10.1007/s11831-018-9259-2

[6] Schillings, C., Schmidt, S., and Schulz, V. "Efficient shape optimization for certain and uncertain aerodynamic design," Computers & Fluids Vol. 46, No. 1, 2011, pp. 78-87.

[7] Allen, M., and Maute, K. "Reliability-based shape optimization of structures undergoing fluid–structure interaction phenomena," Computer Methods in Applied Mechanics and Engineering Vol. 194, No. 30, 2005, pp. 3472-3495.

[8] Du, X., and Chen, W. "Towards a Better Understanding of Modeling Feasibility Robustness in Engineering Design," Journal of Mechanical Design Vol. 122, No. 4, 2000, pp. 385--394.

[9] Blatman, G., and Sudret, B. "Adaptive sparse polynomial chaos expansion based on least angle regression," Journal of Computational Physics Vol. 230, No. 6, 2011, pp. 2345-2367.

[10] Xiu, D., and Karniadakis, G. E. "Modeling uncertainty in flow simulations via generalized polynomial chaos," Journal of Computational Physics Vol. 187, No. 1, 2003, pp. 137-167.

[11] Eldred, M., and Burkardt, J. "Comparison of Non-Intrusive Polynomial Chaos and Stochastic Collocation Methods for Uncertainty Quantification," 47th AIAA Aerospace Sciences Meeting including The New Horizons Forum and Aerospace Exposition. American Institute of Aeronautics and Astronautics, 2009.

[12] Huang, B., and Du, X. "A robust design method using variable transformation and Gauss–Hermite integration," International Journal for Numerical Methods in Engineering Vol. 66, No. 12, 2006, pp. 1841-1858.

[13] Smoljak, S. A. "Quadrature and interpolation formulae on tensor products of certain function classes," Doklady Akademii Nauk Sssr Vol. 4, No. 5, 1963, pp. 240-243.

[14] Xu, H., and Rahman, S. "A generalized dimension‐reduction method for multidimensional integration in stochastic mechanics," International Journal for Numerical Methods in Engineering Vol. 61, No. 12, 2004, pp. 1992-2019.

[15] Jung, D. H., and Lee, B. C. "Development of a simple and efficient method for robust optimization," International Journal for Numerical Methods in Engineering Vol. 53, No. 9, 2002, pp. 2201-2215.

[16] Zhao, H., Gao, Z., Gao, Y., and Wang, C. "Effective robust design of high lift NLF airfoil under multi-parameter uncertainty," Aerospace Science and Technology Vol. 68, 2017, pp. 530-542. doi: 10.1016/j.ast.2017.06.009

[17] Kim, N. H., Wang, H., and Queipo, N. V. "Efficient shape optimization under uncertainty using polynomial chaos expansions and local sensitivities," AIAA Journal Vol. 44, No. 5, 2006, pp. 1112-1116.

[18] Cameron, R. H., and Martin, W. T. "The orthogonal development of non-linear functionals in series of Fourier-Hermite functionals," Annals of Mathematics Vol. 48, No. 2, 1947, pp. 385-392.

[19] Sachdeva, S. K., Nair, P. B., and Keane, A. J. "Hybridization of stochastic reduced basis methods with polynomial chaos expansions," Probabilistic Engineering Mechanics Vol. 21, No. 2, 2006, pp. 182-192.

[20] Perkó, Z., Gilli, L., Lathouwers, D., and Kloosterman, J. L. "Grid and basis adaptive polynomial chaos

techniques for sensitivity and uncertainty analysis," Journal of Computational Physics Vol. 260, No. 3, 2014, pp. 54-84.

[21]Jakeman, J. D., Narayan, A., and Zhou, T. "A generalized sampling and preconditioning scheme for sparse approximation of polynomial chaos expansions," Siam Journal on Scientific Computing Vol. 39, No. 3, 2017.

[22]Peng, J., Hampton, J., and Doostan, A. "A weighted ℓ1-minimization approach for sparse polynomial chaos expansions," Journal of Computational Physics Vol. 267, 2014, pp. 92-111.

[23]Guo, L., Narayan, A., and Zhou, T. "A gradient enhanced ℓ1-minimization for sparse approximation of polynomial chaos expansions," Journal of Computational Physics Vol. 367, 2018, pp. 49-64.

[24]Salehi, S., Raisee, M., Cervantes, M. J., and Nourbakhsh, A. "An efficient multifidelity ℓ1-minimization method for sparse polynomial chaos," Computer Methods in Applied Mechanics & Engineering Vol. 334, 2018, pp. 183-207.

[25]Zhao, H., Gao, Z., Xu, F., and Xia, L. "Adaptive multi-fidelity sparse polynomial chaos-Kriging metamodeling for global approximation of aerodynamic data," Structural and Multidisciplinary Optimization, 2021. doi: 10.1007/s00158-021-02895-2

[26]Palar, P. S., Tsuchiya, T., and Parks, G. T. "Multi-fidelity non-intrusive polynomial chaos based on regression," Computer Methods in Applied Mechanics & Engineering Vol. 305, 2016, pp. 579-606.

[27]Zhao, H., Gao, Z., Xu, F., Zhang, Y., and Huang, J. "An efficient adaptive forward–backward selection method for sparse polynomial chaos expansion," Computer Methods in Applied Mechanics and Engineering Vol. 355, 2019, pp. 456-491.

[28]Palar, P. S., and Shimoyama, K. "On efficient global optimization via universal Kriging surrogate models," Structural and Multidisciplinary Optimization Vol. 57, No. 6, 2018, pp. 2377-2397.

[29]Yan, L., Guo, L., and Xiu, D. "Stochastic collocation algorithms using L1-minimization," International Journal for Uncertainty Quantification Vol. 2, No. 3, 2012, pp. 279-293.

[30]Diaz, P., Doostan, A., and Hampton, J. "Sparse polynomial chaos expansions via compressed sensing and D-optimal design," Computer Methods in Applied Mechanics and Engineering Vol. 336, 2018, pp. 640-666.

[31]Candes, E. J., Romberg, J. K., and Tao, T. "Stable signal recovery from incomplete and inaccurate measurements," Communications on Pure and Applied Mathematics Vol. 59, No. 8, 2006, pp. 1207-1223.

[32]Candès, E. J. "The restricted isometry property and its implications for compressed sensing," Comptes rendus - Mathématique Vol. 346, No. 9, 2008, pp. 589-592.

[33]Rauhut, H., and Ward, R. "Sparse Legendre expansions via ℓ1-minimization," Journal of Approximation Theory Vol. 164, No. 5, 2012, pp. 517-533.

[34]Eldar, Y. C., and Kutyniok, G. Compressed sensing: theory and applications: Cambridge University Press, 2012.

[35]Zhang, T. "Adaptive forward-backward greedy algorithm for learning sparse representations," IEEE transactions on information theory Vol. 57, No. 7, 2011, pp. 4689-4708.

[36]Park, J. S. Tuning complex computer codes to data and optimal designs, 1992.

[37]Ledoux, S. T., Vassberg, J. C., Young, D. P., Fugal, S., Kamenetskiy, D., Huffman, W. P., Melvin, R. G., and Smith, M. F. "Study Based on the AIAA Aerodynamic Design Optimization Discussion Group Test Cases," AIAA Journal Vol. 53, No. 7, 2015, pp. 1-26.

[38]Zhao, H., and Gao, Z. "Robust design optimization of benchmark aerodynamic case based on polynomial chaos expansion," 31st Congress of the International Council of the Aeronautical Sciences, ICAS 2018. 2018.

[39]Zhao, H., Gao, Z., Wang, C., and Yuan, G. "Robust design of high speed natural-laminar-flow airfoil for high lift," 55th AIAA Aerospace Sciences Meeting. 2017, p. 1414.

[40]Zhao, H., Gao, Z., and Gao, Y. "Design Optimization of Natural-Laminar-Flow Airfoil for Complicated Flight Conditions," 35th AIAA Applied Aerodynamics Conference. American Institute of Aeronautics and Astronautics, 2017, p. 3060.

[41]Zhao, H., and Gao, Z. "Uncertainty-based design optimization of NLF airfoil for high altitude long endurance unmanned air vehicles," Engineering Computations Vol. 36, No. 3, 2019, pp. 971-996. doi: doi:10.1108/EC-05-2018-0215

[42]Keane, A. J. "Comparison of several optimization strategies for robust turbine blade design," Journal of Propulsion and Power Vol. 25, No. 5, 2009, p. 1092.

[43]Ghanem, R. G., and Spanos, P. D. "Representation of stochastic processes," Stochastic finite elements: a spectral approach. Springer, 1991, pp. 17-41.